Optical cloaking with metamaterials

WENSHAN CAI, UDAY K. CHETTIAR, ALEXANDER V. KILDISHEV AND VLADIMIR M. SHALAEV*

School of Electrical and Computer Engineering and Birck Nanotechnology Center, Purdue University, West Lafayette, Indiana 47907, USA
*e-mail: shalaev@purdue.edu

Published online: 2 April 2007; doi:10.1038/nphoton.2007.28

Artificially structured metamaterials have enabled unprecedented flexibility in manipulating electromagnetic waves and producing new functionalities, including the cloak of invisibility based on coordinate transformation[1–3]. Unlike other cloaking approaches[4–6], which are typically limited to subwavelength objects, the transformation method allows the design of cloaking devices that render a macroscopic object invisible. In addition, the design is not sensitive to the object that is being cloaked. The first experimental demonstration of such a cloak at microwave frequencies was recently reported[7]. We note, however, that that design[7] cannot be implemented for an optical cloak, which is certainly of particular interest because optical frequencies are where the word 'invisibility' is conventionally defined. Here we present the design of a non-magnetic cloak operating at optical frequencies. The principle and structure of the proposed cylindrical cloak are analysed, and the general recipe for the implementation of such a device is provided.

The coordinate transformation used in the proposed non-magnetic optical cloak of cylindrical geometry is similar to that in ref. 7, by which a cylindrical region $r < b$ is compressed into a concentric cylindrical shell $a < r < b$ as shown in Fig. 1a. This transformation results in the following requirements for anisotropic permittivity and permeability in the cloaking shell[7,8]:

$$\varepsilon_r = \mu_r = \frac{r-a}{r}, \quad \varepsilon_\theta = \mu_\theta = \frac{r}{r-a}, \quad \varepsilon_z = \mu_z = \left(\frac{b}{b-a}\right)^2 \frac{r-a}{r} \qquad (1)$$

where ε is the dielectric permittivity, μ is the magnetic permeability and the subscripts r, θ and z denote radial, azimuthal and z-axis alignment respectively.

For transverse-electric (TE) illumination, where the incident electrical field is polarized along the z-axis, only ε_z, μ_r and μ_θ in equation (1) enter into Maxwell's equations. Moreover, the dispersion properties and wave trajectory in the cloaking shell remain the same, as long as the values of $\varepsilon_i\mu_z$ and $\mu_i\varepsilon_z$ are kept constant, where i represents either r or θ. This has all been addressed in the recent microwave experiments[7], where cloaking was achieved by varying the dimensions of a series of split-ring resonators (SRRs) to yield a desired gradient of permeability in the radial direction. However, this approach cannot be used for an optical cloak. It is a known fact that there are intrinsic limits to the scaling of SRR size in order to exhibit a magnetic response in the optical range[9,10]. Replacing the SRRs with other optical magnetic structures such as paired nanorods[11] or nanostrips[12] is also very challenging, because magnetism based on such resonant plasmonic structures is usually associated with a high loss factor, which is detrimental to the performance of cloaking devices.

In contrast to the reported design of a microwave cloak with TE polarization[7], we focus on transverse magnetic (TM) incidence, with the magnetic field polarized along the z-axis. In this case only μ_z, ε_r and ε_θ must satisfy the requirements in equation (1), and the dispersion relations inside the cloak remain unaffected as long as the products of $\mu_z\varepsilon_r$ and $\mu_z\varepsilon_\theta$ are kept the same as those determined by the values in equation (1). It is worth noting that under TM illumination, only one component of μ is of interest, which allows us to completely remove the need for any optical magnetism. In equation (1) we multiply ε_r and ε_θ by the value of μ_z and obtain the following reduced set of cloak parameters:

$$\mu_z = 1, \quad \varepsilon_\theta = \left(\frac{b}{b-a}\right)^2, \quad \varepsilon_r = \left(\frac{b}{b-a}\right)^2 \left(\frac{r-a}{r}\right)^2 \qquad (2)$$

Compared to the cloak with ideal properties as shown in equation (1), the reduced parameters in equation (2) provide the same wave trajectory. The only adverse effect of using the reduced set is the non-zero reflection due to the impedance mismatch at the outer boundary. The ideal parameters in equation (1) result in a perfectly matched impedance of $Z = \sqrt{(\mu_z/\varepsilon_\theta)} = 1$ at $r = b$, whereas the reduced set in equation (2) produces an impedance at the outer boundary of $Z = 1 - R_{ab}$, where $R_{ab} = a/b$ denotes the ratio between the inner and outer radii. Therefore, the level of power reflection due to reduced parameters can be estimated as $|(1 - Z)/(1 + Z)|^2 = [R_{ab}/(2 - R_{ab})]^2$.

The non-magnetic nature of the system as indicated in equation (2) removes the most challenging issue of the design. The azimuthal permittivity is a constant, with a magnitude larger than 1, which can be easily achieved in conventional dielectrics. The key to the implementation is to construct the cylindrical shell with the desired radial distribution of ε_r varying from 0 at the inner boundary of the cloak ($r = a$) to 1 at the outer surface ($r = b$). In our design, the required distribution of ε_r is realized by using metal wires of subwavelength size in the radial direction, embedded in a dielectric material, as shown in Fig. 1b. The aspect ratio of the metal wires, defined by the ratio of the length to the radius of the wire, is denoted by α. The spatial positions of the wires do not have to be periodic and can be random. The electromagnetic response of such metal wires can be characterized by the screening factor κ, which indicates the strength of the interaction between the field and the wire. The effective permittivity ε_{eff} for a composite material comprising metal particles with permittivity ε_{m}, a volume filling factor f and screening factor κ, along with a dielectric component with permittivity ε_{d} and a filling factor $1 - f$, is given by the

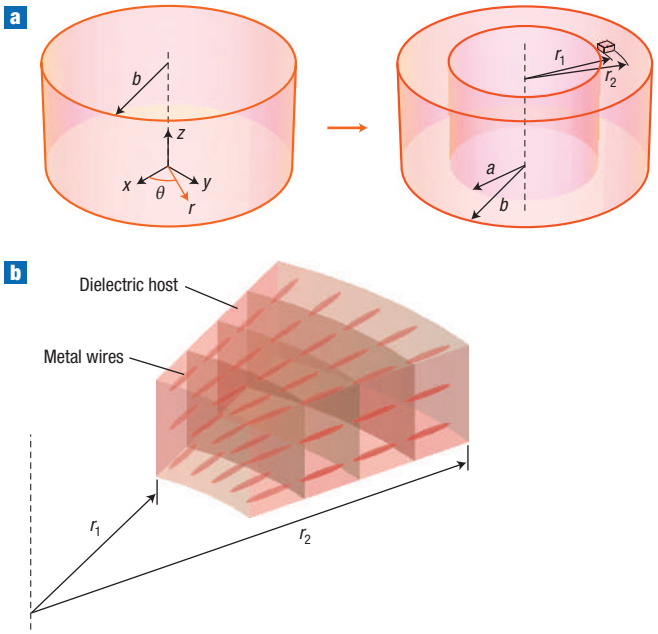

Figure 1 Coordinate transformation and structure of the non-magnetic optical cloak. a, The coordinate transformation that compresses a cylindrical region $r < b$ into a concentric cylindrical shell $a < r < b$. There is no variation along the z direction. r_1 and r_2 define the internal and external radius of a fraction of the cylindrical cloak. **b**, A small fraction of the cylindrical cloak. The wires are all perpendicular to the cylinder's inner and outer interfaces, but their spatial positions do not have to be periodic and can be random. Also, for large cloaks, the wires can be broken into smaller pieces that are smaller in size than the wavelength.

'shape-dependent' effective-medium theory (EMT) (see, for example, ref. 13):

$$\varepsilon_{\text{eff}} = \frac{1}{2\kappa}\left\{\bar{\varepsilon} \pm \sqrt{\bar{\varepsilon}^2 + 4\kappa\varepsilon_{\text{m}}\varepsilon_{\text{d}}}\right\} \tag{3}$$

where $\bar{\varepsilon} = [(\kappa+1)f - 1]\varepsilon_{\text{m}} + [\kappa - (\kappa+1)f]\varepsilon_{\text{d}}$.

The benefit of using metal wires in a composite cloak is that the radial permittivity ε_r determined by equation (3) may exhibit a positive value less than 1 with a minimal imaginary part. For the structure in Fig. 1b, the filling fraction in equation (3) for calculating ε_r is $f(r) = f_a \cdot (a/r)$, with f_a being the filling fraction of metal at the inner surface of the cloak. The azimuthal permittivity ε_θ inside the cloak is essentially the same as that of the dielectric, because the response of the wires to the angular electrical field E_θ oriented normal to the wires is small, and at low metal filling factors it can be neglected.

The reduced set of cloak parameters in equation (2) requires a smooth variation of the radial permittivity from 0 to 1 as r changes from a to b. For optimal performance the effective radial permittivity, $\varepsilon_{\text{eff},r}$ should exactly follow the function described in (2) such that

$$\varepsilon_{\text{eff},r}\left(f_a \cdot \frac{a}{r}\right) = \left(\frac{b}{b-a}\right)^2\left(\frac{r-a}{r}\right)^2 \tag{4}$$

In a practical design, $\varepsilon_{\text{eff},r}$ is allowed to have some discrepancy from the optimal value inside the cloak. The most important points are

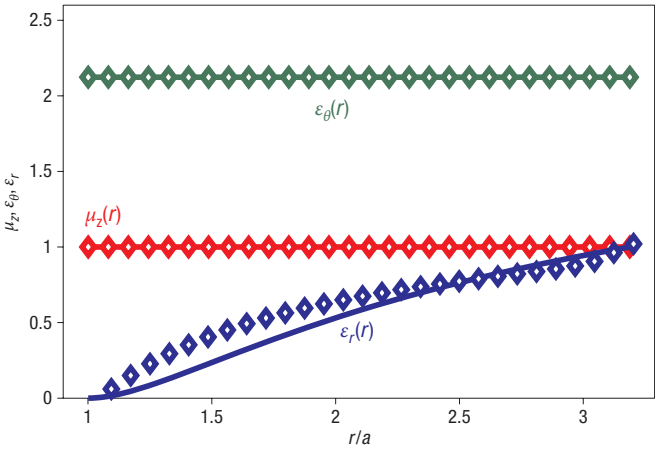

Figure 2 Material parameters ε_r, ε_θ and μ_z of the proposed cloak operating at $\lambda = 632.8$ nm. The solid lines represent the exact set of reduced parameters determined by equation (2). The diamond markers show the material properties of the designed metal wire composite cloak with parameters obtained from equations (3) to (8).

at the inner and outer surfaces of the cloak, where equation (4) should be satisfied exactly. This ensures the desired wave trajectory at $r = b$ and the minimum leakage energy at $r = a$.

To determine all of the parameters of the design shown in Fig. 1b, we define two filling-fraction functions $f_0(\lambda, \alpha)$ and $f_1(\lambda, \alpha)$, such that for given constituent composite materials and a wire aspect ratio of α, the effective radial permittivity is

$$\begin{cases} \varepsilon_{\text{eff},r}(\lambda, f_0(\lambda,\alpha)) = 0 \\ \varepsilon_{\text{eff},r}(\lambda, f_1(\lambda,\alpha)) = 1 \end{cases} \tag{5}$$

Combining equations (4) and (5), at the operational wavelength λ we obtain

$$\begin{cases} f_0(\lambda,\alpha) = f_a \\ f_1(\lambda,\alpha) = f_a \cdot a/b \end{cases} \tag{6}$$

Hence we can express the shape factor R_{ab} as

$$R_{ab} = a/b = f_1(\lambda,\alpha)/f_0(\lambda,\alpha) \tag{7}$$

Using equation (7) with the expression for ε_θ in equation (2), we obtain the operating condition of the cloak:

$$\varepsilon_\theta(\lambda) = \left(\frac{f_0(\lambda,\alpha)}{f_0(\lambda,\alpha) - f_1(\lambda,\alpha)}\right)^2 \tag{8}$$

For practical applications, it is important to design a cloaking device operating at a preset operational wavelength λ_{op}. For this purpose, the design process is as follows. First we choose materials for the metal wires and the surrounding dielectric. Second, we calculate the values of f_0 and f_1 as functions of the aspect ratio α at λ_{op} using the EMT model in equation (3). The required aspect ratio for λ_{op} is the one that satisfies equation (8). Then, the geometrical factors of the cloak, including R_{ab} and f_a, can be determined based on equations (6) and (7). Note that the same design works for all similar cylindrical cloaks with the same shape factor R_{ab}.

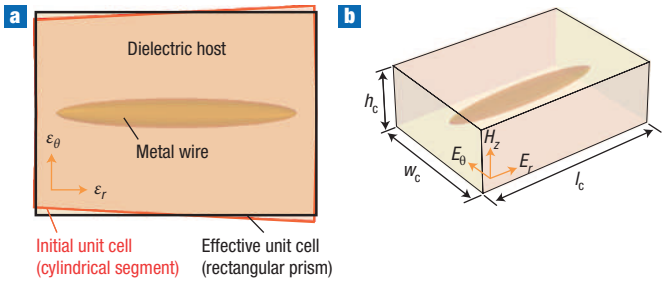

Figure 3 Unit cell for full-wave FE simulations of effective parameters. **a**, The actual unit cell (cylindrical sector) encapsulating a spheroidal silver wire is substituted by a cell made of a right rectangular prism. **b**, The geometry of the three-dimensional rectangular unit cell. In simulations h_c and l_c are fixed, and w_c changes in proportion to the radius of each layer.

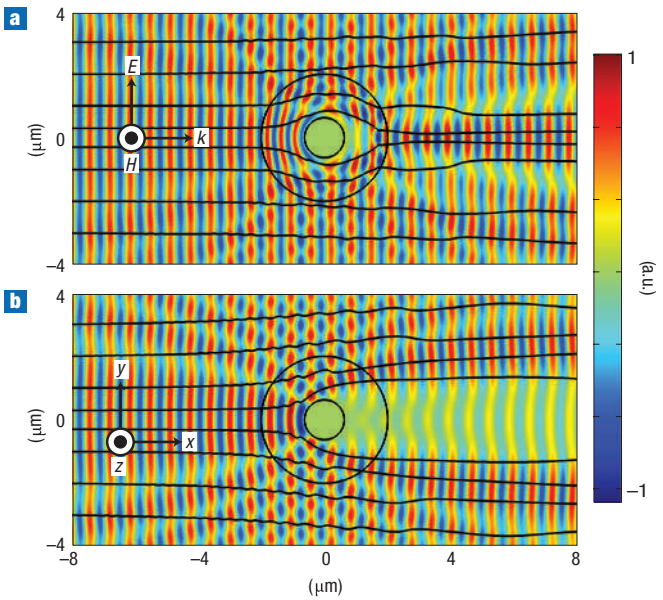

Figure 4 FE simulations of the magnetic-field mapping around the cloaked object with TM illumination at λ = 632.8 nm. **a**, The object is inside the designed metal-wire composite cloak with parameters given by the diamond markers in Fig. 2 where *H* is the magnetic field, *E* is the electric field and k is the wave vector. **b**, The object is surrounded by vacuum without the cloak. The concentric circles represent the two boundaries of the cloak at $r = a$ and $r = b$, respectively. The hidden object is an ideal metallic cylinder with radius $r = a$.

As a practical example, we have designed an optical cloak operating at the wavelength of 632.8 nm (that of a He–Ne laser) and consisting of silver and silica. Equations (3), (5) and (8) together yield the desired aspect ratio $\alpha = 10.7$, and the filling fractions at the two boundaries are $f_a = 0.125$ and $f_b = 0.039$, respectively. Then, with equations (6) and (7), we find the shape factor of the cylindrical cloak to be $R_{ab} = 0.314$. The effective parameters of μ_z, ε_r and ε_θ from this design, together with the exact set of reduced parameters determined by equation (2), are shown in Fig. 2. We can see that μ_z and ε_θ perfectly match the theoretical requirements throughout the cylindrical cloak. The radial permittivity ε_r fits the values required by equation (2) exactly at the two boundaries of the cloak, and follows the overall trend very well inside the cloak.

To validate if the required distribution of permittivity could be achieved using prolate spheroidal silver nanowires embedded in a silica tube, we determine the effective anisotropic permittivity of a unit cell with subwavelength dimensions. We start with a homogenization method[7], where the actual unit cells (cylindrical sectors) with different electromagnetic surroundings are substituted by cells made of right-rectangular prisms, as shown in Fig. 3. The full-wave finite-element (FE) numerical analysis confirms that the range of desired ε_r and ε_θ fits rather well with those predicted by EMT. The FE modelling also shows that the dependence of ε_r and ε_θ can match exactly those required by equation (2) through additional adjustment of the aspect ratio and the volume fraction of the nanowires in each layer (see Methods section). As for the loss feature, the FE simulations show that the radial permittivity ε_r has an imaginary part of about 0.1 throughout the cloak. Although this is a very small value for metal–dielectric metamaterials, it may still weaken the cloaking effect. It is possible to compensate the loss by using a gain medium as already proposed for applications of perfect tunnelling transmittance[5] and lossless negative-index materials[14,15].

To illustrate the performance of the proposed non-magnetic optical cloak with a design corresponding to Fig. 2 at $\lambda_{op} = 632.8$ nm, we performed field-mapping simulations using a commercial FE package (COMSOL Multiphysics). The object hidden inside the cloak is an ideal metallic cylinder with radius $r = a$. The simulated results of magnetic-field distribution around the cloaked object together with the power flow lines are illustrated in Fig. 4. We note that the size of the cloak is more than 6 times the operational wavelength, and the simulated area is more than 20 times larger than the wavelength. Figure 4a shows the field distribution around the metal cylinder surrounded by the designed cloak, with parameters given by the diamond markers in Fig. 2. With the cloak (Fig. 4a), the wave fronts flow around the cloaked region with remarkably small perturbation, but without the cloak (Fig. 4b) the waves around the object are severely distorted and an evident shadow is cast behind the cylinder. In the designed system with $R_{ab} = 0.314$, the estimated power reflection is about 4% when one uses the reduced set of parameters given by equation (2). This is a low level of reflection, and the small value is consistent with what we observe in simulations (see Supplementary Information, Fig. S1b). Thus, our simulations clearly show the capability of reducing the scattering from the object hidden inside the cloaked region.

We have demonstrated a design of an optical cloak based on coordinate transformation. The non-magnetic nature of our design eases the pain of constructing gradient magnetic metamaterials in three-dimensional space, and therefore paves the way for the realization of cloaking devices at optical frequencies. The proposed design can be generalized to cloaks with other metal structures, such as chains of metal nanoparticles or thin continuous or semicontinuous metal strips. It can also be adopted for ranges other than the optical spectral ranges, including the infrared and the microwave. We note that the achievable invisibility with the proposed cloak is not perfect due to the impedance mismatch associated with the reduced material specifications and the inevitable loss in a metal–dielectric structure. Moreover, any shell-type cloak design can work only over a narrow frequency range, because the curved trajectory of light implies a refractive index n of less than 1 in order to satisfy the minimal optical path requirement of Fermat's principle, and any metamaterial with $n < 1$ must be dispersive to fulfill causality. However, we believe that even rudimentary designs and

implementations of an optical cloak are of great potential interest and bring us one step closer to the ultimate optical illusion of invisibility.

METHODS

SHAPE-DEPENDENT EFFECTIVE-MEDIUM THEORY

The shape-dependent electromagnetic response of a subwavelength particle can be characterized by the Lorentz depolarization factor q. For an ellipsoid having semiaxes a_i, a_j and a_k with electric field polarized along a_i, the depolarization factor is expressed by[16]

$$q_i = \int_0^\infty \frac{a_i a_j a_k \, \mathrm{d}s}{2(s+a_i^2)^{3/2}(s+a_j^2)^{1/2}(s+a_k^2)^{1/2}}$$

The screening factor κ of a particle is related to q by $\kappa = (1-q)/q$. Note that a long wire with large α results in small q and a large κ, which indicates strong interactions between the field and the wires. For a composite cloak with metal wires as inclusions in a dielectric, the electromagnetic properties are well-described by 'shape-dependent' effective-medium theory (EMT). The effective permittivity for a composite material comprising metal particles with permittivity ε_m, a volume filling factor f and screening factor κ, along with a dielectric component with permittivity ε_d and a filling factor $1-f$, is given by[17]

$$f\frac{\varepsilon_m - \varepsilon_{eff}}{\varepsilon_m + \kappa\varepsilon_{eff}} + (1-f)\frac{\varepsilon_d - \varepsilon_{eff}}{\varepsilon_d + \kappa\varepsilon_{eff}} = 0 \qquad (9)$$

For spherical particles with $q = 1/3$ and $\kappa = 2$, the equation above reduces to the common EMT expression[17,18]. The solution to equation (9) is given by equation (3), and the sign in equation (3) should be chosen such that $\varepsilon''_{eff} > 0$.

FINITE-ELEMENT SIMULATIONS FOR EFFECTIVE PARAMETERS

Full-wave simulations with the commercial finite-element solver COMSOL Multiphysics are used to test the effective parameters of the proposed structure. The unit cells used for the calculation are shown in Fig. 3a. The curvature of the actual unit cells is relatively low; thus we assume that converting the cylindrical segment into the rectangular prism introduces minuscule changes to the ε_{eff}. The effective permittivity of the unit cells has been obtained from a three-dimensional finite element (FE) model. For a wavelength of 632.8 nm, we fix two dimensions of the unit cell (height, $h_c = 12.5$ nm and length, $l_c = 100$ nm), while changing the width w_c proportional to the radius of each layer. The FE simulations show that for the equivalent rectangular unit cell encapsulating a spheroidal silver nanowire with the dimensions initially calculated through EMT (diameter $d = 7$ nm and length $l = 75$ nm), the effective permittivity ε_r fits relatively well with the desired values, with a discrepancy of around 10%. The required effective material properties can be achieved more precisely by additionally adjusting the diameter of the rod to $d = 6$ nm ($d = 5$ nm), and length to $l = 71$ nm ($l = 60$ nm) for the external (internal) cell. In this case the material parameters are $\varepsilon_r = 1.0$ and $\varepsilon_\theta = 2.3$ ($\varepsilon_r = 0.0$ and $\varepsilon_\theta = 2.4$) for the external (internal) cell; that is, they closely match the desired values. We note that $\varepsilon''_r \approx 0.1$, $\varepsilon''_\theta \approx 0.0$ and $\mu_z = 1.0$ for both cells. The homogenization of the two limiting cases proves good control over the effective material properties of the unit cell in the proposed cloak.

FIELD-MAPPING SIMULATIONS

The simulation approach for field mapping shown in Fig. 4 is similar to that in ref. 8, but with the important difference that our cloaking device is designed for optical wavelengths with TM incident light instead of the transverse-electric mode at microwave frequencies. The simulations were carried out using the FE solver (COMSOL). The simulation model consisted of the cylindrical cloak identical to the one shown in Fig. 1 with TM-polarized waves. The simulation domain also consisted of perfectly matched layers at all the boundaries to absorb the outgoing waves.

Received 20 November 2006; accepted 19 February 2007; published 2 April 2007.

References

1. Pendry, J. B., Schurig, D. & Smith, D. R. Controlling electromagnetic fields. *Science* **312,** 1780–1782 (2006).
2. Leonhardt, U. Optical conformal mapping. *Science* **312,** 1777–1780 (2006).
3. Leonhardt, U. Notes on conformal invisibility devices. *New J. Phys.* **8,** 118 (2006).
4. Alu, A. & Engheta, N. Achieving transparency with plasmonic and metamaterial coatings. *Phys. Rev. E* **72,** 016623 (2005).
5. Garcia de Abajo, F. J., Gomez-Santos, G., Blanco, L. A., Borisov, A. G. & Shabanov, S. V. Tunneling mechanism of light transmission through metallic films. *Phys. Rev. Lett.* **95,** 067403 (2005).
6. Milton, G. W. & Nicorovici, N.-A. P. On the cloaking effects associated with anomalous localized resonance. *Proc. R. Soc. A* **462,** 3027–3059 (2006).
7. Schurig, D. *et al.* Metamaterial electromagnetic cloak at microwave frequencies. *Science* **314,** 977–980 (2006).
8. Cummer, S. A., Popa, B.-I., Schurig, D., Smith, D. R. & Pendry, J. Full-wave simulations of electromagnetic cloaking structures. *Phys. Rev. E* **74,** 036621 (2006).
9. Zhou, J. *et al.* Saturation of the magnetic response of split-ring resonators at optical frequencies. *Phys. Rev. Lett.* **95,** 223902 (2005).
10. Klein, M. W., Enkrich, C., Wegener, M., Soukoulis, C. M. & Linder, S. Single-slit split-ring resonators at optical frequencies: limits of size scaling. *Opt. Lett.* **31,** 1259–1261 (2006).
11. Podolskiy, V. A., Sarychev, A. K. & Shalaev, V. M. Plasmon modes in metal nanowires and left-handed materials. *J. Nonlin. Phys. Mater.* **11,** 65–74 (2002).
12. Kildishev, A. V. *et al.* Negative refractive index in optics of metal–dielectric composites. *J. Opt. Soc. Am. B* **23,** 423–433 (2006).
13. Shalaev, V. M. *Nonlinear Optics of Random Media: Fractal Composites and Metal-Dielectric Films* (Springer, Berlin, 2000).
14. Chettiar, U. K. *et al.* From low-loss to lossless optical negative-index materials. *CLEO/QELS-06 Annual Meeting Proceedings*, Long Beach, California, May 21–26 (2006).
15. Klar, T. A., Kildishev, A. V., Drachev, V. P. & Shalaev, V. M. Negative-index metamaterials: Going optical. *IEEE J. Sel. Top. Quant. Electron.* **12,** 1106–1115 (2006).
16. van de Hulst, H. C. *Light Scattering by Small Particles* (Dover, New York, 1981).
17. Aspnes, D. E. Optical properties of thin films. *Thin Solid Films* **89,** 249–262 (1982).
18. Bruggeman, D. A. G. Berechnung verschiedener physikalischer konstanten von heterogenen substanzen. *Ann. Phys.* **416,** 636–679 (1935).

Acknowledgement

This work was supported in part by ARO-MURI award 50342-PH-MUR.
Supplementary information accompanies this paper on www.nature.com/naturephotonics.

Competing financial interests

The authors declare that they have no competing financial interests.

Supplementary Information

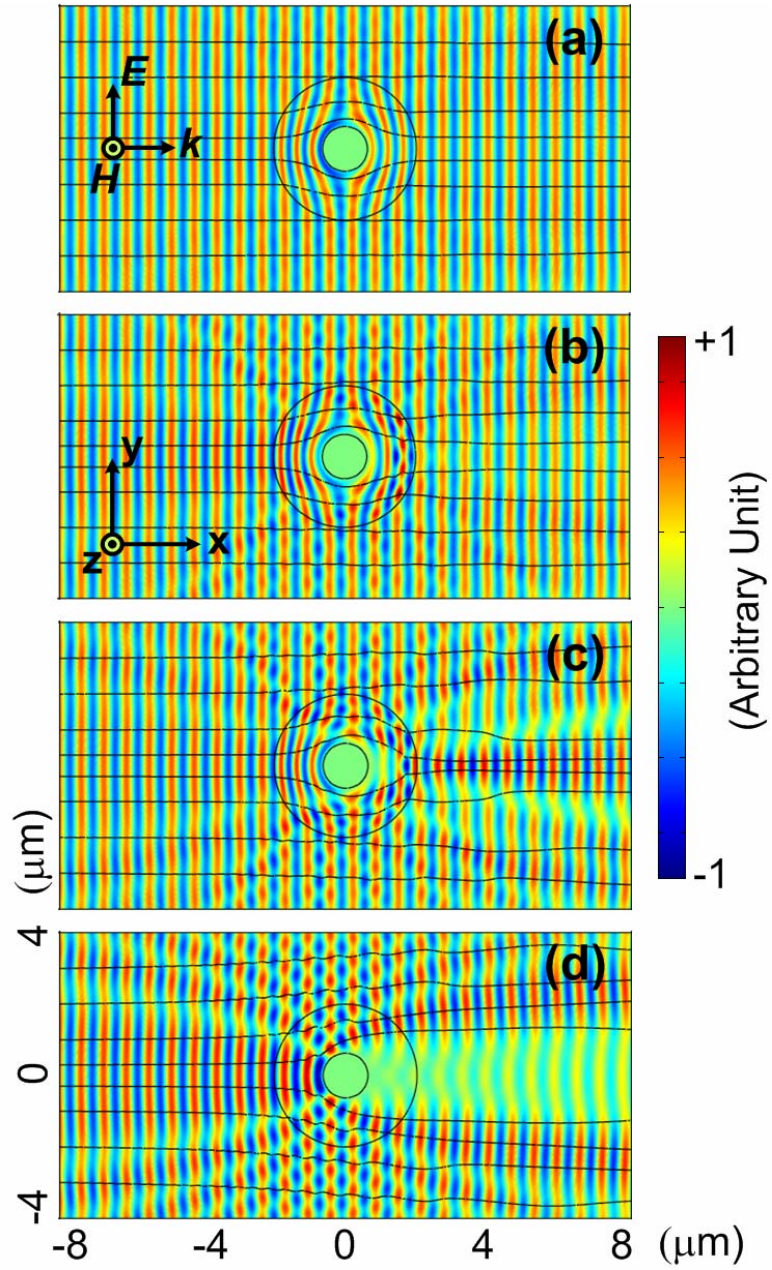

Supplementary Figure 1. Full wave finite-element simulations of the magnetic field mapping around the cloaked object surrounded by: a, ideal cloak with parameters determined by equation (1); **b,** non-magnetic cloak with parameters given by equation (2); **c,** the designed metal wire composite cloak with parameters given by the diamond markers in Fig. 2; **d,** vacuum wave propagation without the cloak. All size parameters and illumination conditions are identical to those in Fig. 4.